Article

PS9, Derived from an Aquatic Fungus Virulent Protein, Glycosyl Hydrolase, Arrests MCF-7 Proliferation by Regulating Intracellular Reactive Oxygen Species and Apoptotic Pathways

Manikandan Velayutham, Purabi Sarkar, Kanchana M. Karuppiah, Priyadharsan Arumugam, Shanavas Shajahan, Mohammad Abu Haija, Tansir Ahamad, Mariadhas Valan Arasu, Naif Abdullah Al-Dhabi, Ki-Choon Choi, Ajay Guru,* and Jesu Arockiaraj*

Cite This: *ACS Omega* 2023, 8, 18543−18553
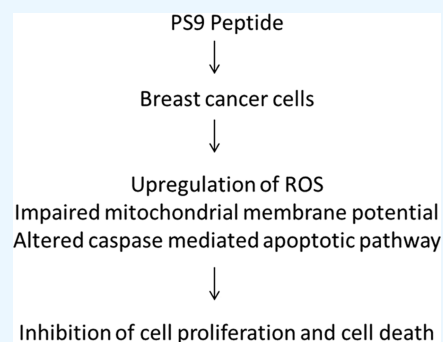
Read Online

ACCESS | ◫ Metrics & More | ◫ Article Recommendations | ◫ Supporting Information

ABSTRACT: One of the most common diseases in women is breast cancer, which has the highest death globally. Surgery, chemotherapy, hormone treatments, and radiation are the current treatment options for breast cancer. However, these options have several adverse side effects. Recently, peptide-based drugs have gained attention as anticancer therapy. Studies report that peptides from biological toxins such as venom and virulent pathogenic molecules have potential therapeutic effects against multiple diseases, including cancers. This study reports on the *in vitro* anticancer effect of a short peptide, PS9, derived from a virulent protein, glycosyl hydrolase, of an aquatic fungus, *Aphanomyces invadans*. This peptide arrests MCF-7 proliferation by regulating intercellular reactive oxygen species (ROS) and apoptotic pathways. Based on the potential for the anticancer effect of PS9, from the *in silico* analysis, *in vitro* analyses using MCF-7 cells were executed. PS9 showed a dose-dependent activity; its IC_{50} value was 25.27−43.28 μM at 24 h. The acridine orange/ethidium bromide (AO/EtBr) staining, to establish the status of apoptosis in MCF-7 cells, showed morphologies for early and late apoptosis and necrotic cell death. The 2,7-dichlorodihydrofluorescein diacetate (DCFDA) staining and biochemical analyses showed a significant increase in reactive oxygen species (ROS). Besides, PS9 has been shown to regulate the caspase-mediated apoptotic pathway. PS9 is nontoxic, *in vitro*, and *in vivo* zebrafish larvae. Together, PS9 may have an anticancer effect *in vitro*.

PS9 Peptide
↓
Breast cancer cells
↓
Upregulation of ROS
Impaired mitochondrial membrane potential
Altered caspase mediated apoptotic pathway
↓
Inhibition of cell proliferation and cell death

1. INTRODUCTION

Bioactive peptides have been considered pharmacological alternatives in treating cancers. Studies show that peptides synthesized from various resources, including microbes, plants, and animals, have exhibited antimicrobial, antioxidant, and anticancer properties.[1] Small molecules, including peptides, are considered a distinct group of pharmacological compounds for their specific biochemical and therapeutic properties. Peptides have been developed as therapeutic candidates to disrupt protein−protein interactions (PPIs) and target intercellular molecules.[2] In a peptide, the combination of amino acids, sequence arrangement, number of amino acids, structural configuration, hydrophobicity, net charge, isoelectric point, and molecular mass contributes to the anticancer nature.[3] There are about 80 peptide-based commercial drugs with therapeutic potential. One hundred and fifty peptides are under clinical trials, and 600 are in preclinical testing.[4]

Cancers have been considered a significant global barrier to survival rates.[5,6] The Cancer Research Center in the United Kingdom has reported that the prevalence rate of cancer could increase to 62% by 2040.[4] Breast cancer, the most common type of cancer in women, affects one in every four women, and its mortality rate has increased to 11.7% of all cancer cases.[5] Since "reactive oxygen species (ROS)" and "cancer" refer to a wide range of substances and conditions, broad generalizations are almost unattainable. However, is it possible to characterize the redox status of cancer in terms of any shared characteristics? There is a common misconception that practically all malignant cells are pro-oxidative, mostly because oncogenes modify and accelerate cell metabolism.[6]

Small molecules, such as peptides and compounds from toxin origin, have significant biological functions, including antimicrobial, antioxidant, and anticancer. The structurally modified synthetic peptide, VmCT1, developed from the α-helical region of *Vaejovis mexicanus* smithi (the scorpion's venom), showed antimicrobial activity against MCF-7 cells.[7] Further, ICD-85, a venom-derived peptide, promoted
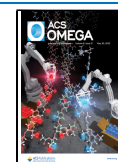
apoptosis in the MCF-7 cells by activating the caspase signals.[8] *Aspergillus fumigatus* (invasive aspergillosis causing pathogenic fungus)-derived small molecule elicited anticancer activity.[9] MP12, derived from the virulent fungal molecule trypsin inhibitor, showed significant anticancer properties against human laryngeal cancer cells (Hep-2).[10] The *in vivo* toxicity of the virulent peptide was screened in the zebrafish embryo model. The zebrafish model has been extensively used in biology, pharmacology, drug development, cancer, and toxicology studies. A zebrafish model activated with H_2O_2 has been used by several researchers to study the antioxidant capabilities of compounds.[11] Models made from zebrafish or embryos offer many advantages, including size, transparency, quick development, and minimal maintenance expenses. Zebrafish species have a genomic similarity to the human genome and the pathophysiology of human disease of about 85% compared to other model organisms.[12]

The virulent molecule glycosyl hydrolase has been identified from our earlier established transcriptome database on fish disease-causing pathogenic fungus *Aphanomyces invadans*.[13,14] Glycosyl hydrolases are a common class of enzymes that break down the glycosidic link between two or more carbs or between a carbohydrate and a noncarbohydrate component. The establishment of 85 distinct families is the result of a classification scheme for glycosyl hydrolases based on sequence similarity.[15,16]

This study investigated the anticancer property of PS9 derived from fungal glycosyl hydrolase. *In vitro* analyses including neutral red uptake assay, apoptosis staining, 2,7-dichlorodihydrofluorescein diacetate (DCFDA) staining, Rhodomine123 assay, the status of biochemical enzymes (superoxide dismutase (SOD), catalase (CAT), glutathione peroxidase (GPx), glutathione *S*-transferase (GST), and glutathione (GSH)), and quantitative polymerase chain reaction (qPCR) analysis of apoptotic genes were carried out using MCF-7 cells. Toxicity assays were performed for PS9 under *in vitro* (Madin−Darby canine kidney (MDCK) cells) and *in vivo* (zebrafish embryo) conditions.

2. MATERIALS AND METHODS

2.1. *In Silico* Analysis for PS9 and Peptide Synthesis.
The cDNA sequence of the virulent protein glycosyl hydrolase was identified from the previously established transcriptome of the epizootic ulcerative syndrome (EUS) or red spot disease (in teleost fish) causing pathogenic fungus *A. invadans*. The identified cDNA sequence was analyzed using the ExPASy tool (http://web.expasy.org/translate/) to convert the cDNA to protein.[17] The converted protein sequence was analyzed on the NCBI BLAST, program, and the homology has been established. The properties of the peptide were analyzed using Expasy's ProtParam online tool (http://us.expasy.org/tools/protparam.html).[18] A three-dimensional (3D) structure of the predicted protein was established using I-The ASSER webserver and visualized over PyMol (ver. 0.99).[17]

The peptide sequence and properties were predicted using the HeliQuest online tool (http://heliquest.ipmc.cnrs.fr/cgi-bin/ComputParams.py).[19] The peptide's toxicity was predicted using the ToxIBTL online tool (http://server.wei-group.net/ToxIBTL).[20] The anticancer property of the peptide was screened using the webserver AntiCP 2.0 (https://webs.iiitd.edu.in/raghava/anticp2).[21]

The peptide was synthesized at Zhengzhou Peptides Pharmaceutical Technology Co. Ltd., China. The supplier certified that the peptide is >95% purity as per the high-performance liquid chromatography (HPLC)-mass spectrometry analysis. A stock solution (1 mM) of the peptide was prepared by dissolving it in phosphate-buffered saline (PBS), and the working concentrations (10, 20, 30, 40, and 50 μM) were prepared before the treatment. The prepared stock was stored at −20 °C until further use.[22]

2.2. Anticancer Potency of PS9. *2.2.1. Maintenance of Cells.*
Human dermal fibroblast (HDF, Passage No.: 19) and breast cancer cells (MCF-7 Passage No.: 21) were procured from the National Centre for Cell Science (NCCS), Pune, India. The maximum passage no range used experiment was HDF cell line-24 and MCF-7 cell line-29. The cells were grown as a monolayer with Dulbecco's modified Eagle's essential medium (DMEM, 4.5 g/L high glucose, Gibco, U.K.) containing 10% fetal bovine serum (FBS) (heat-inactivated fetal bovine serum, Gibco, U.K.) and 100 U/mL of penicillin and streptomycin (Sigma-Aldrich). The cells were maintained at 5% CO_2 and 37 °C.

2.2.2. Neutral Red Uptake Assay. To determine the antiproliferative effect of PS9 against the MCF-7 cell, a neutral red uptake assay has been performed as per the previous protocol.[23] Briefly, the cells were seeded in a 96-well plate and grown until 90% confluency, followed by the peptide treatment at different concentrations for 24−48 h. Untreated cells served as control. Cells were washed three times with sterile PBS, and then 0.4% of neutral red solution (Sigma-Aldrich) was added and incubated for 3 h in the dark at room temperature. Cells were then washed, destained (50% ethanol and 1% glacial acetic acid), and incubated for 30 min. The absorbance at 540 nm was read using a MultiSkan Go ELISA reader (Thermofisher Scientific, Finland). Cell viability was calculated as absorbance obtained. The log dose−response curve and 50% inhibitory concentration (IC50) were established using GraphPad Prism software Ver 5.03 (CA).

2.2.3. Measurement of PS9 on Lactate Dehydrogenase (LDH) Release. The potential of the peptide to cause cell membrane damage was carried out in MCF-7 cells by determining the level of lactose dehydrogenase enzyme released by the cells. Cells were seeded in six-well plates and allowed to reach 90% confluency, followed by the peptide treatment for 24−48 h. Untreated cells served as a control, while the Triton-X-100-treated cells served as a positive control. The culture medium and cell lysate measured the total LDH level. Parallelly, cells were inoculated with 50 μL of pyruvic acid (4.6 mM, prepared in 0.1 M potassium phosphate buffer of pH 7.4) in a 96-well plate, which was followed by the addition of 50 μL of reduced nicotinamide adenine dinucleotide (NADH) (0.5 mg/mL). The absorbance values were recorded at 340 nm for 2 min using a MultiSkan Go ELISA reader (Thermofisher Scientific, Finland), and the concentration of the released LDH was calculated.[24,25]

2.2.4. Morphological and Apoptotic Assessment Using Acridine Orange/Ethidium Bromide (AO/EtBr) Stain. MCF-7 cells (1×10^6 cells/well) were plated in a six-well plate and grown until they reached 90% confluency. Cells were then exposed to different peptide concentrations (between 10 and 50 μM) for 24 h. Changes in the cell morphology were observed at 20× magnification under an inverted microscope.[26] Treated cells were stained with 20 μL of fluorescent dye (100 μg/mL acridine orange (AO) + 100 μg/mL ethidium bromide (EtBr) at a 1:1 ratio) for 20 min. Cells were then washed with PBS and visualized under a fluorescence

Table 1. List of Primers Used for the Anticancer Gene Expression Study

gene		primer sequence	reference
BAX	forward	5′-TCAGGATGCGTCCACCAAGAAG-3′	38
	reverse	5′-TGTGTCCACGGCGGCAATCATC-3′	
Bcl-2	forward	5′-GTGGATGACTGAGTACCT-3′	
	reverse	5′-CCAGGAGAAATCAAACAGAG-3′	
caspase-3	forward	5′-ACATGGAAGCGAATCAATGGACTC-3′	
	reverse	5′- AAGGACTCAAATTCTGTTGCCACC-3′	
caspase-9	forward	5′-GCTCTTCCTTTGTTCATC- 3′	
	reverse	5′- CTCTTCCTCCACTGTTCA-3′	
GAPDH (internal control)	forward	5′-GTCTCCTCTGACTTCAACAGCG-3′	
	reverse	5′-ACCACCCTGTTGCTGTAGCCAA-3′	

microscope, and the results were recorded as photomicrographs.[27]

2.2.5. Measurement ROS by DCFDA Staining. DCFDA staining assay detected the changes in the concentration of intracellular ROS.[28−30] MCF-7 cells (1×10^6 cells/well) were seeded in a six-well plate and allowed to reach 90% confluency, and the cells were treated with various peptide concentrations (between 10 and 50 μM) for 24 h. Untreated cells were considered as a control. Following the peptide exposure, cells were stained with 20 μg/mL of 2,7-dichlorodihydrofluorescein diacetate (DCFDA) and incubated in the dark for 20 min. Then, cells were washed with PB to remove the excess stain and examined under the fluorescence microscope at 20× magnification. Results were recorded as images, and the fluorescent intensity was determined using ImageJ software (v.1.49, NIH).

2.2.6. Mitochondrial Membrane Potential of PS9. The ability of the peptide to influence the mitochondrial membrane potential was determined, as reported previously.[31] MCF-7 cells were seeded in a six-well plate and allowed to reach 80% confluency. Cells were treated with different peptide concentrations for 24 h. Untreated cells served as a control. The peptide-exposed cells were then stained with rhodamine 123 (10 μg/mL) and incubated in the dark for 20 min. To remove the excess stain, cells were washed three times with PBS. Results were recorded as photomicrographs by examination under the fluorescence microscope (20× magnification). ImageJ software (V.1.49, NIH) measured the fluorescent intensity.

2.2.7. Biochemical Estimation. To determine the effect of PS9 in regulating the cellular components, enzyme activities of antioxidant enzymes (superoxide dismutase (SOD), catalase (CAT), glutathione (GSH)) and the extent of lipid peroxidation were established.[32−34] For the antioxidant enzyme activity, changes in the absorbance values were measured using a UV−visible spectrophotometer (UV 1800, SHIMADZU, Japan). Briefly, MCF-7 cells (1×10^6 cells/well) were seeded in a six-well plate and allowed to grow until 80% confluency. Cells were then exposed to different peptide concentrations for 24 h, as mentioned elsewhere. Cells were scraped, homogenized using 100 mM tris−HCl buffer (pH 7.4), and centrifuged for 5 min at 8000g. A supernatant was utilized to estimate the enzyme activity. To determine the glutathione level, scraped cells were homogenized in sulfosalicylic acid (5%) and centrifuged at 4000g for 12 min; the homogenate served as a source of glutathione.

2.2.8. Gene Expression of PS9. Gene expression analysis was performed to understand the molecular mechanism(s) by which PS9 elicits an anticancer effect. MCF-7 cells (1×10^6 cells/well) were seeded in a six-well plate, grown until 80% confluency, and treated with different concentrations such as 20 and 40 μM of PS9 peptide for 24 h. Untreated cells were considered as a control. Total RNA was isolated by scrapping the cells in a TRIZOL reagent as per the manufacturer's instructions (BioLit, SRL, India).[35−37] Gene expression analysis was performed using a KAPA SYBR FAST one-step qRT-PCR master mix kit in the Light cycler 96 (Roche Diagnostics, GmbH, Germany) along with the respective primers (Table 1). Data were calculated using the $2^{-\Delta\Delta Ct}$ method, and the results were expressed as relative folds.[38−40]

2.3. Toxicity Analysis of PS9. *2.3.1. In Vitro Cytotoxic Activity of PS9.* The ability of the peptide to elicit a cytotoxic effect was evaluated using the 3-(4,5-dimethylthiazol-2-yl)-2,5-diphenyltetrazolium bromide (MTT) assay.[22,41,42] HDF cells (95×10^3 cells/well) were seeded in a 96-well plate and allowed to grow until 90% confluency. The experimental group received PS9 at different concentrations, whereas the control received no PS9 and the positive control received Triton-X-100. After the peptide exposure, cells were incubated with MTT reagent (20 μL of 5 mg/mL; 3-(4,5-dimethylthiazol-2-yl)-2,5-diphenyltetrazolium bromide; Sigma-Aldrich) for 4 h in the dark at room temperature. Culture media was removed after incubation, and dimethyl sulfoxide (DMSO) was added; the absorbance was then read at 650 nm using a MultiSkan Go ELISA reader (Thermofisher Scientific, Finland).

2.3.2. In Vivo Developmental Toxicity Due to PS9 in Zebrafish Embryo. Zebrafish (wild adult) were obtained from a local vendor in Chennai, Tamil Nadu, India. As previously mentioned, fish have maintained in a glass aquaria and acclimatized.[22,32,43] Zebrafish embryo toxicity was performed according to OECD guidelines. Four-hour postfertilized (hpf) embryos were taken in a six-well plate (30 embryos/well) and exposed to PS9 at different concentrations, diluted in fish water or E3 medium. Peptide exposure was semistatic, and 50% of the exposure solution was renewed every 24 h and the concentration range of 10, 20, 30, and 40 μM. The developmental toxicity including hatching rate, heart rate, mortality, survival rate, and morphology was analyzed.[44−47] When 48 h had passed since fertilization, the hatching rate was measured. The numbers of dead and alive larvae were counted, and the percentages of mortality and survival were calculated. Larvae were chosen at random from the group, and the heart's systolic and diastolic rhythms were observed under a light microscope. In each group, the step was performed three times while the heartbeat was counted and recorded. At several stages, 24, 48, 72, and 96 hpf, the embryo morphology was investigated under a light microscope and the results were recorded as the picture.
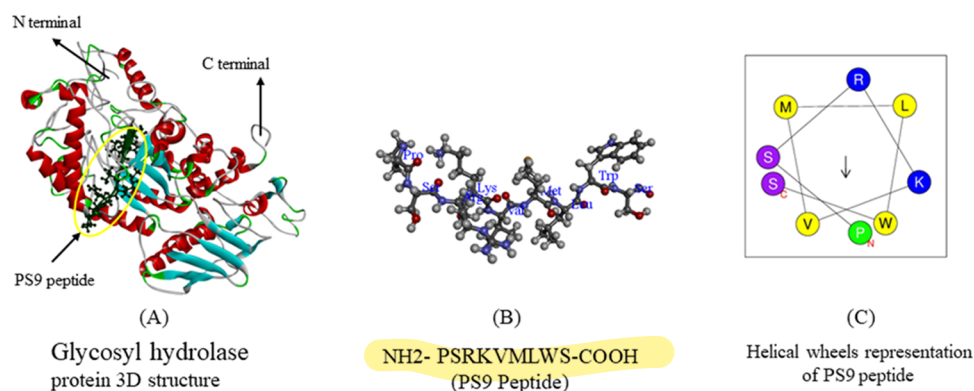
Figure 1. *In silico* investigation of glycosyl hydrolase protein and its derived PS9. (A) 3D structure of the glycosyl hydrolase protein. (B) 3D structure of the PS9 peptide. (C) Hydrophobicity analysis in the helical wheel analysis.
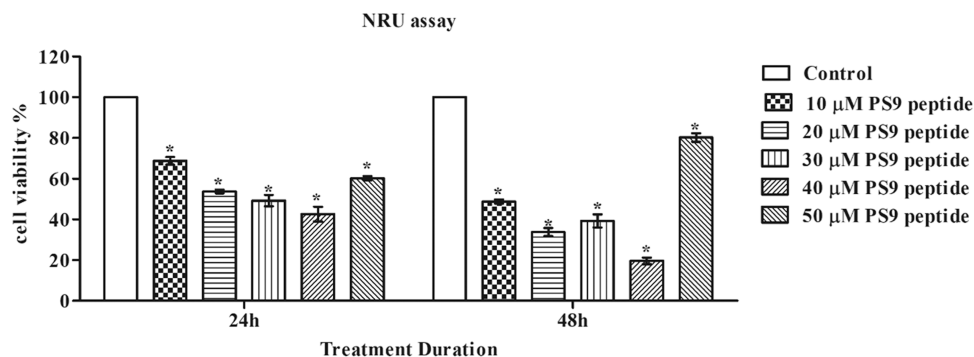

Figure 2. Anticancer potency of PS9 due to neutral red uptake assay. The results were compared with the control, and the data were expressed as mean ± SD. The asterisk (*) represents the statistical significance at $p < 0.05$.

2.4. Statistics.

The data presented in the study are the mean of three replicates and their standard deviation (SD). GraphPad Prism (ver. 5.0) has been utilized to identify the significance of the data through one-way analysis of variance (ANOVA) and post hoc Tukey's multiple range test.

3. RESULTS AND DISCUSSION

The venom of snakes, bees, scorpions, animals, and plant pathogenic fungal-derived virulence factors are examples of toxic components that have been found to have a potential anticancer effect.[4,23,48,49] Peptide molecules elicit the anticancer effect by targeting multiple cellular mechanisms, including immune modulation, inhibition of distinct internal targets, apoptosis, and tumor angiogenesis suppression.[50,51] The peptide, PS9, has been derived from the virulent protein, glycosyl hydrolase (Figure 1A), of the fungus *A. invadans*. The physicochemical properties of the protein are as follows: molecular mass, 74.45 kDa; theoretical point, 6.40; the total number of negatively (Asp + Glu) and positively charged residues (Arg + Lys) in the protein, 72 and 66, respectively; chemical formula of the protein, $C_{3313}H_{5125}N_{911}O_{968}S_{39}$; estimated half-life, 30 h (mammalian reticulocytes, *in vitro*), 20 h (yeast, *in vivo*), and 10 h (*Escherichia coli*, *in vivo*); instability index, 36.99; aliphatic index, 80.00; and grand average of hydropathicity of the protein (GRAVY), −0.193. The derived peptide, PS9 (Figure 1B,C), has nine amino acid residues: ^{NH2}Pro−Ser−Arg−Lys−Val−Met−Leu−Trp−Ser^{COOH}. The estimated physicochemical properties of PS9 are molecular mass, 1103.34 g/mol; extinction coefficient, 5690 M^{-1} cm^{-1}; isoelectric point, 11.52; net charge at pH, 7: 2; hydrophobicity, 0.560; hydrophobic moment, 0.275; the

number of uncharged residues, 2 SER; aromatic residue, 1 TRP; charged residues, 1 LYS and 1 ARG; and special residue, 1 PRO. The *in silico* analysis of PS9 has predicted that the peptide is nontoxic as its score was 5.88296×10^{-12}. The anticancer property of PS9, as predicted through AntiCP 2.0, has a score of 0.49. Overall, the *in silico* analysis indicated that PS9 might be a lead anticancer peptide (ACP) or a molecule with the characteristics of the ACP, as described.[3,52] Further, the amino acids such as TRP, LYS, ARG, and PRO present in PS9 play a significant role in the bioactivity against the survival of cancer cells.[3]

Neutral red is a positively charged dye that diffuses through the plasma membranes to accumulate in the lysosomes. Therefore, the intracellular intensity of the dye due to its intracellular accumulation is directly proportional to the percentage of living cells.[25] PS9-challenged MCF-7 cells showed a significant ($p > 0.05$) dose-dependent reduction in the percentage of cell viability, except at 50 μM of PS9, wherein relatively lesser activity has been observed (Figure 2). The assay was performed at two different time intervals; however, similar results were observed at both time points. Results indicate that the IC$_{50}$ value range at 24 h is between 25.27 and 43.28 μM, whereas at 48 h, the value is between 9.9 and 37.5 μM. Based on the neutral red uptake assay, it states that the PS9 peptide inhibits the MCF-7 cell proliferation.

LDH assay revealed the cytotoxic potency of PS9 in MCF-7 cells. PS9 challenge showed that the total LDH percentages were 39.28 ± 1.9% at 10 μM followed by 47.86 ± 3.2% at 20 μM, 57.62 ± 1.4% at 30 μM, 71.25 ± 1.3% at 40 μM, and 40.75 ± 2.3% at 50 μM in 24 h. Moreover, when the duration of the peptide exposure was increased to 48 h, the total LDH
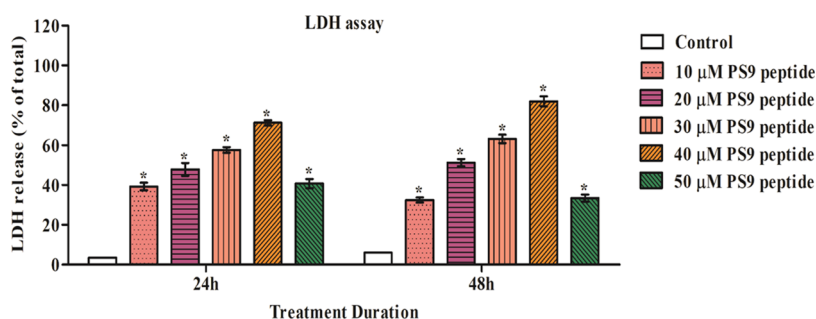
Figure 3. Total LDH release due to the PS9 treatment on MCF-7 cells. The data were compared with the untreated control. The data showed a significant difference at $p < 0.05$, which was indicated by an asterisk (*). The data were presented as the mean of three replicates ± SD.
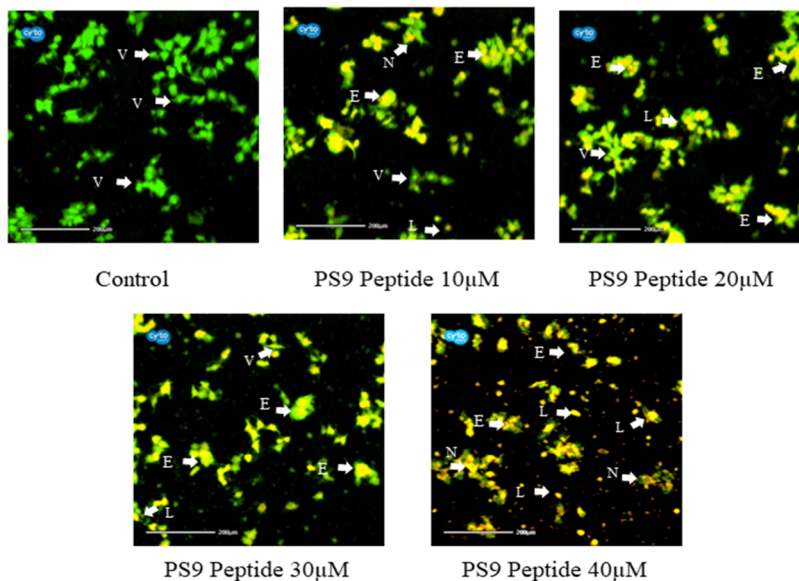

Figure 4. Morphological analysis of PS9-treated cells at 20× magnifications in an inverted phase-contrast microscope. Both the circles and arrows represent the abnormal morphology of the cells.
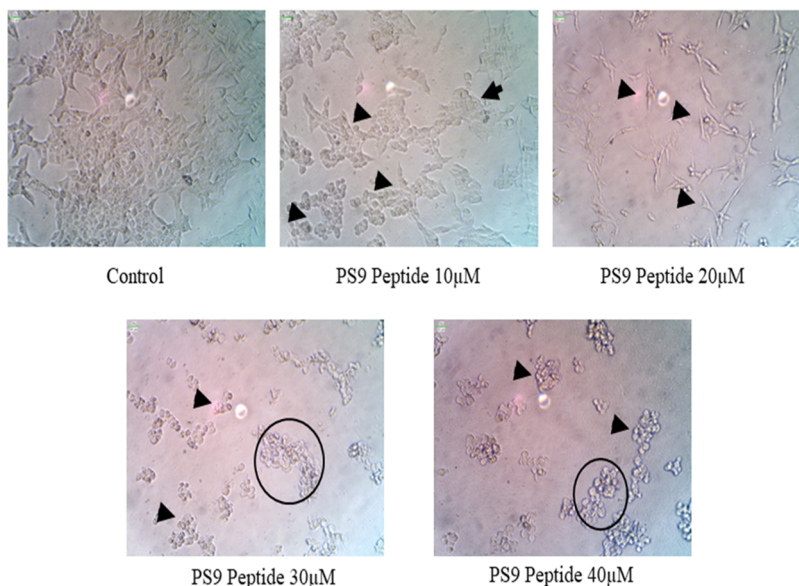

Figure 5. Acridine orange/ethidium bromide (AO/EtBr) staining on MCF-7 cells to analyze the apoptotic stages. V, viable cells; E, early apoptotic cells; L, late apoptotic cells; and N, necrotic cells.

levels were as follows: 32.48 ± 1.3% at 10 μM, 51.24 ± 1.8% at 20 μM, 63.12 ± 2.1% at 30 μM, 81.98 ± 2.5% at 40 μM, and 30.45 ± 1.8% at 50 μM. In both the peptide exposure durations, there was a dose-dependent increment in the LDH

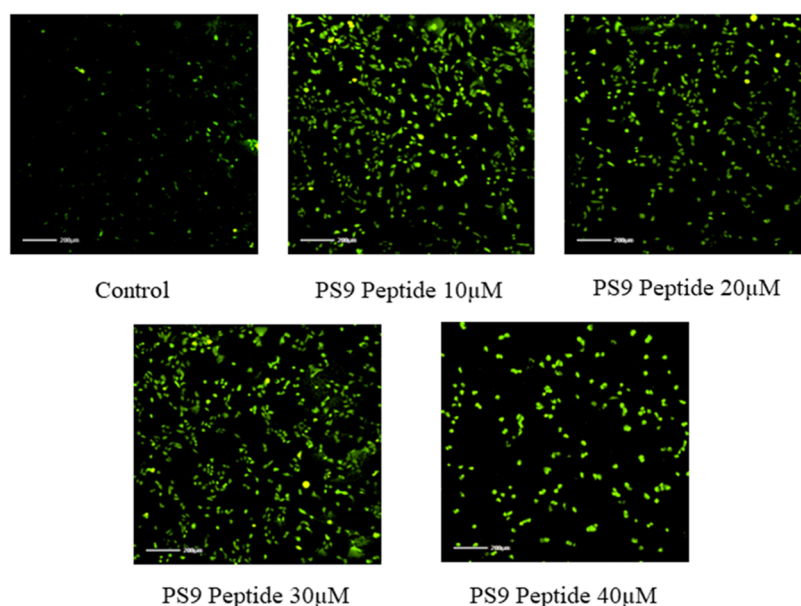Control   PS9 Peptide 10μM   PS9 Peptide 20μM

PS9 Peptide 30μM   PS9 Peptide 40μM

Figure 6. DCFDA staining to measure the ROS level on MCF-7 cells. PS9 treatment generates ROS compared to the untreated control.

Control   PS9 Peptide 10μM   PS9 Peptide 20μM
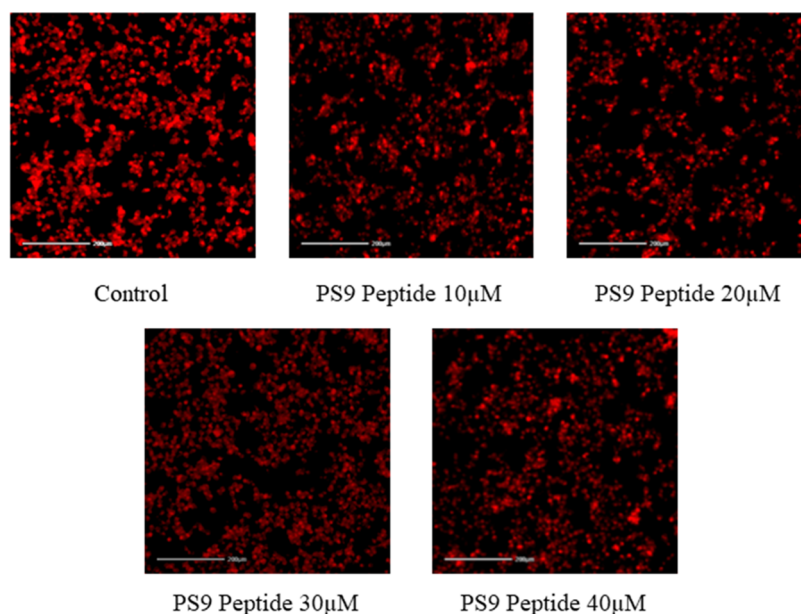
PS9 Peptide 30μM   PS9 Peptide 40μM

Figure 7. Mitochondrial membrane potentiality of PS9. The PS9 treatment showed a dose-dependent activity on MCF-7 cells compared to the untreated control.

levels. However, at a 50 μM peptide concentration, in both time points, there was a reduction in LDH activity (Figure 3). Similar observations have been reported previously in (i) *A. invadans* virulence protein, trypsin inhibitor-derived peptide inhibited human laryngeal cancer[10] and (ii) *Brevibacillus laterosporus* isolated peptide, brevilaterin B that increases the LDH level, has been utilized to address epidermal cancer.[53] Based on this supporting evidence and the outcomes of this study, we suggest that PS9 inhibits MCF-7 cell proliferation at a concentration range between 10 and 40 μM. It is possible that the reduced activity at a higher (50 μM) peptide concentration could be due to the saturation point of the peptide. Based on the neutral red assay, LDH assay, and IC$_{50}$ value, further anticancer experiments were followed with a 10–40 μM concentration.

PS9-treated MCF-7 cells showed abnormal morphology including cell shrinkage, granulation of cells, cell rounding, loss of rigidness, and detachment from the culture flask (Figure 4). Similar observations have been reported previously from a peptide that was extracted from *Grapsus albacarinous*, which is known to affect the cell morphology in MCF-7 cells.[54] Based on this observation, we suggest that PS9 compromises the cellular morphology, which could pave the way for the cells to undergo apoptosis. Based on the fluorescent emissions in the AO/EtBr analysis, different apoptotic stages have been identified, including early apoptosis (yellow), late apoptosis (reddish-brown), necrosis (brown), and viable cells (green) (Figure 5). These observations are in line with the previous reports, wherein nymphayol was found to promote apoptosis in MCF-7 cells.

Table 2. Effects of PS9 on the Antioxidant Proteins and Its Lipid Peroxidation Level in MCF-7 Cells[a]

groups	SOD (units/mg proteins)	CAT (units/mg proteins)	GSH (units/mg proteins)	LPO (MDA level) (mM/mg protein)
control	29.27 ± 1.32	16.71 ± 2.32	31.73 ± 2.32	12.47 ± 2.32
10 μM	26.38 ± 1.1	15.79 ± 2.1	25.74 ± 5.4	19.36 ± 3.1*
20 μM	17.27 ± 1.3*	12.87 ± 3.2*	16.45 ± 2.3*	28.75 ± 2.1*
30 μM	12.98 ± 3.32*	9.89 ± 2.1*	11.35 ± 3.2*	37.31 ± 1.2*
40 μM	7.61 ± 5.1*	9.72 ± 1.2*	9.23 ± 1.32*	52.36 ± 4.2*

[a]The asterisk (*) represents the statistical significance at $p < 0.05$. Results were compared with the control group, and values are expressed as mean ± SD ($n = 3$).
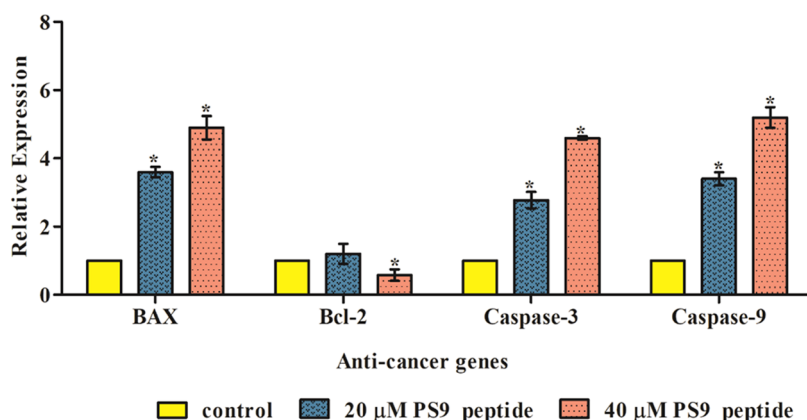

Figure 8. Gene expression analysis of PS9 on MCF-7 cells. The expression was calculated after the data were normalized with GAPDH. The data were expressed as mean ± SD of three independent experiments. The asterisk (*) denotes the significance level at $p < 0.05$ compared to the control.

In addition, the PS9 challenge upregulated the intracellular ROS concentration in a dose-dependent manner in MCF-7 cells[38] (Figures 6 and S1). In support of this observation on ROS generation, AMK1 has been reported to significantly increase ROS production in cancer cells.[55]

Rhodamine 123 has been utilized to measure the effect of PS9 on the mitochondrial membrane potential in MCF-7 cells. Results demonstrate that there is a dose-dependent activity (Figures 7 and S2). The peptide-exposed cells had more substantial activity than the untreated control. According to Siddiqui et al.,[56] mitochondrial damage is triggered by increased intracellular ROS. Moreover, the obtained results are in line with a dipeptide from *Callyspongia fstularis* (marine sponge) symbiont *Bacillus pumilus*, which showed that an increase in ROS concentration leads to mitochondrial damage. Therefore, we suggest that PS9 targets mitochondrial membrane potential to cause damage to cancer cells.

Oxidation of membrane-bound lipids, which is triggered by excessive intracellular ROS generation, may change the status of the antioxidant enzymes to eventually degrade MMP.[57] Likewise, PS9-challenged MCF-7 cells show increased ROS levels, which eventually causes mitochondrial damage. Moreover, PS9 treatment showed a dose-dependent reduction in the levels of antioxidant enzymes including SOD, CAT, and GSH. In line with this outcome, there was a dose-dependent increase in the lipid peroxidation level (Table 2). One study has reported on a similar trend, wherein ferruginol challenge to MCF-7 cells influenced the levels of antioxidant enzymes and LPO enzymes by enhancing the intracellular ROS generation.[58]

Increased ROS led to accelerated DNA damage and cell death by mitigating the mitochondrial membrane potential, releasing cytochrome *c*, activating caspase-3, upregulating BAX,

and downregulating Bcl-2 expression (Figure 8) in PS9-treated MCF-7 cells. Such an interesting outcome has been previously demonstrated.[59] PS9-challenged MCF-7 cells, at 20 and 40 μM, showed a dose-dependent upregulation on the expression of BAX, caspase-3, and caspase-9. However, the peptide treatment appears to downregulate the expression of Bcl-2. Similar observations have been reported previously, wherein VS-9 peptide from *Allium sativum* induced caspase-3- and caspase-9-mediated apoptosis against leukemic cells.[60]

We examined the toxicity of PS9 using *in vitro* (HDF cells) and *in vivo* (zebrafish embryo) models because PS9 has been derived from a pathogenic fungal virulence protein, glycosyl hydrolase. *In vitro* toxicity experiment using PS9 showed that the cell viability values are 91.02 ± 3.2% at 10 μM, 84.13 ± 2.9% at 20 μM, 81.13 ± 4.5% at 30 μM, and 81.06 ± 2.5% at 40 μM concentration, whereas the untreated cells showed a 100% cell viability and the positive control Triton-X-100 (0.01%) showed 19.12 ± 1.9%. These outcomes indicate that PS9 is nontoxic to healthy cells (Figure S3). In our previous study,[22] we reported that NV14 peptides derived from cyanobacteria also showed nontoxicity.

Compared to other *in vivo* models, the zebrafish model offers a variety of significant advantages.[61] The developmental toxicity assay was performed in zebrafish using embryos between 4 and 96 hpf. PS9 treatment did not induce any significant changes in the hatching rate, heart rate, mortality, and survival rate. However, at 40 μM concentration, PS9 showed slight variation in these said parameters. Exposure to (1 mM) hydrogen peroxide showed a significant difference in the hatching rate. According to the hatching rate results, the PS9 peptide did not affect any embryo hatching rates; nevertheless, the group that was exposed to H_2O_2 had lower hatching rates (Figure S4). The embryos exposed to 10−40

μM of the PS9 peptide showed a similar death rate to the control as did the H_2O_2-treated embryos, which had the greatest mortality rates (Figure S4). The heart rate and normal morphology of the embryos were not altered in the PS9 peptide-exposed group, nevertheless. The H_2O_2 (1 mM)-exposed embryos had aberrant heart rates and morphological defects such as bent tails and bent spines (BS) (Figure S4). Also, PS9 did not have any influence on the morphology of the embryo (Figure 9). A similar observation has been reported in

Figure 9. Toxicity study on zebrafish larvae between 0 and 72 hpf. The larvae were treated with four different concentrations of PS9. The untreated larvae were considered the control, and the larvae treated with 1 mM of H_2O_2 were considered the positive control. The positive control showed abnormal morphologies such as a bent spine (BS).

the peptide, MP12, derived from *A. invadans* virulent molecule, a cysteine-rich trypsin inhibitor treated on human laryngeal epithelial cells.[10] Hence, in the *in vitro* and *in vivo* models, PS9 is nontoxic.

4. CONCLUSIONS

To sum up, based on the *in silico* outcomes for PS9 that the peptide could have anticancer properties, *in vitro* analyses were executed. Results showed that PS9 inhibits the cell proliferation of MCF-7 cells by upregulating the intracellular ROS concentration, regulating the antioxidant enzymes, and through the caspase-mediated apoptotic pathway. Although PS9 has been derived from the pathogenic fungal virulent protein, the peptide is nontoxic in *in vitro* and *in vivo* models. Therefore, we suggest that PS9 could be a promising anticancer agent.

ASSOCIATED CONTENT

ⓢ Supporting Information

The Supporting Information is available free of charge at https://pubs.acs.org/doi/10.1021/acsomega.3c00336.

PS9 peptide activity on regulating ROS and apoptosis was identified through the fluorescent staining assay; further, their fluorescent intensity was measured to obtain a quantitative ROS and apoptosis levels; also, the toxic effect of the peptide was investigated in both the *in vitro* and *in vivo* conditions (PDF)
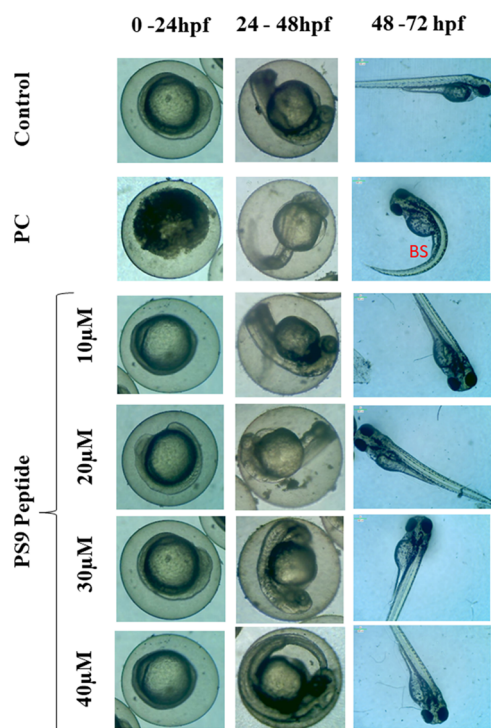
■ AUTHOR INFORMATION

Corresponding Authors

Ajay Guru − *Department of Conservative Dentistry and Endodontics, Saveetha Dental College and Hospitals, SIMATS, Chennai 600077 Tamil Nadu, India;* ⓞ orcid.org/0000-0002-8583-9352; Email: ajayguru.sdc@saveetha.com

Jesu Arockiaraj − *Department of Biotechnology, College of Science and Humanities, SRM Institute of Science and Technology, Chennai 603203 Tamil Nadu, India;* Email: jesuaroa@srmist.edu.in

Authors

Manikandan Velayutham − *Department of Medical Biotechnology and Integrative Physiology, Institute of Biotechnology, Saveetha School of Engineering, Saveetha Institute of Medical and Technical Sciences, Chennai 602105 Tamil Nadu, India*

Purabi Sarkar − *Department of Molecular Medicine, School of Allied Healthcare and Sciences, Jain Deemed-to-be University, Bangalore 560066 Karnataka, India*

Kanchana M. Karuppiah − *Department of Medical Research, Medical College Hospital and Research Centre, SRM Institute of Science and Technology, Chennai 603203 Tamil Nadu, India*

Priyadharsan Arumugam − *Department of Conservative Dentistry and Endodontics, Saveetha Dental College and Hospitals, SIMATS, Chennai 600077 Tamil Nadu, India*

Shanavas Shajahan − *Department of Conservative Dentistry and Endodontics, Saveetha Dental College and Hospitals, SIMATS, Chennai 600077 Tamil Nadu, India; Department of Chemistry, Khalifa University of Science and Technology, 127788 Abu Dhabi, United Arab Emirates;* ⓞ orcid.org/0000-0001-9711-7165

Mohammad Abu Haija − *Department of Chemistry, Khalifa University of Science and Technology, 127788 Abu Dhabi, United Arab Emirates; Center for Catalysis and Separations, Khalifa University of Science and Technology, 127788 Abu Dhabi, United Arab Emirates;* ⓞ orcid.org/0000-0002-5846-0662

Tansir Ahamad − *Department of Chemistry, College of Science, King Saud University, Riyadh 11451, Saudi Arabia*

Mariadhas Valan Arasu − *Department of Botany and Microbiology, College of Science, King Saud University, Riyadh 11451, Saudi Arabia*

Naif Abdullah Al-Dhabi − *Department of Botany and Microbiology, College of Science, King Saud University, Riyadh 11451, Saudi Arabia*

Ki-Choon Choi − *Grassland and Forage Division, National Institute of Animal Science, RDA, Cheonan-Si, Chungnam 330-801, Republic of Korea*

Complete contact information is available at:
https://pubs.acs.org/10.1021/acsomega.3c00336

Author Contributions

M.V., P.S., K.M.K., and P.A. performed most of the experiments and wrote the manuscript. S.S., M.A.H., T.A., M.V.A., N.A.A.-D., and K.-C.C. reviewed and edited the manuscript. A.G. and J.A. supervised and validated the work.

Notes

The authors declare no competing financial interest.

■ ACKNOWLEDGMENTS

■ REFERENCES

(1) Wang, L.; Dong, C.; Li, X.; Han, W.; Su, X. Anticancer potential of bioactive peptides from animal sources. *Oncol. Rep.* **2017**, *38*, 637−651.

(2) Lee, A. C. L.; Harris, J. L.; Khanna, K. K.; Hong, J. H. A comprehensive review on current advances in peptide drug development and design. *Int. J. Mol. Sci.* **2019**, *20*, No. 2383.

(3) Chiangjong, W.; Chutipongtanate, S.; Hongeng, S. Anticancer peptide: Physicochemical property, functional aspect and trend in clinical application (Review). *Int. J. Oncol.* **2020**, *57*, 678−696.

(4) Mikaelian, A. G.; Traboulay, E.; Zhang, X. M.; Yeritsyan, E.; Pedersen, P. L.; Ko, Y. H.; Matalka, K. Z. Pleiotropic anticancer properties of scorpion venom peptides: Rhopalurus princeps venom as an anticancer agent. *Drug Des., Dev. Ther.* **2020**, *14*, 881−893.

(5) Sung, H.; Ferlay, J.; Siegel, R. L.; Laversanne, M.; Soerjomataram, I.; Jemal, A.; Bray, F. Global Cancer Statistics 2020: GLOBOCAN Estimates of Incidence and Mortality Worldwide for 36 Cancers in 185 Countries. *CA—Cancer J. Clin.* **2021**, *71*, 209−249.

(6) Vucetic, M.; Cormerais, Y.; Parks, S. K.; Pouysségur, J. The Central Role of Amino Acids in Cancer Redox Homeostasis: Vulnerability Points of the Cancer Redox Code. *Front. Oncol.* **2017**, *7*, No. 319.

(7) Pedron, C. N.; Silva, A. F.; Torres, M. D. T.; de Oliveira, C. S.; Andrade, G. P.; Cerchiaro, G.; Pinhal, M. A. S.; Fuente-Nunez, C.; Junior, V. X. O. Net charge tuning modulates the antiplasmodial and anticancer properties of peptides derived from scorpion venom. *J. Pept. Sci.* **2021**, *27*, No. e3296.

(8) Zarandi, P. K.; Mirakabadi, A. Z.; Sotoodehnejadnematalahi, F. Cytotoxic and anticancer effects of ICD-85 (Venom derived peptides) in human breast adenocarcinoma and normal human dermal fibroblasts. *Iran. J. Pharm. Res.* **2019**, *18*, 232−240.

(9) Yin, W.-B.; Baccile, J. A.; Bok, J. W.; Chen, Y.; Keller, N. P.; Schroeder, F. C. A Nonribosomal Peptide Synthetase-Derived Iron(III) Complex from the Pathogenic Fungus *Aspergillus fumigatus*. *J. Am. Chem. Soc.* **2013**, *135*, 2064−2067.

(10) Velayutham, M.; Sarkar, P.; Rajakrishnan, R.; Kuppusamy, P.; Juliet, A.; Arockiaraj, J. Antiproliferation of MP12 derived from a fungus, *Aphanomyces invadans* virulence factor, cysteine-rich trypsin inhibitor on human laryngeal epithelial cells, and in vivo zebrafish embryo model. *Toxicon* **2022**, *210*, 100−108.

(11) Wang, L.; Oh, J. Y.; Kim, H. S.; Lee, W. W.; Cui, Y.; Lee, H. G.; Kim, Y. T.; Ko, J. Y.; Jeon, Y. J. Protective effect of polysaccharides from Celluclast-assisted extract of Hizikia fusiforme against hydrogen peroxide-induced oxidative stress in vitro in Vero cells and in vivo in zebrafish. *Int. J. Biol. Macromol.* **2018**, *112*, 483−489.

(12) Naomi, R.; Bahari, H.; Yazid, M. D.; Embong, H.; Othman, F. Zebrafish as a Model System to Study the Mechanism of Cutaneous Wound Healing and Drug Discovery: Advantages and Challenges. *Pharmaceuticals* **2021**, *14*, No. 1058.

(13) Kumaresan, V.; Pasupuleti, M.; Arasu, M. V.; Al-Dhabi, N. A.; Arshad, A.; Amin, S. M. N.; Yusoff, F. D.; Arockiaraj, J. A comparative transcriptome approach for identification of molecular changes in

Aphanomyces invadans infected *Channa striatus*. *Mol. Biol. Rep.* **2018**, *45*, 2511−2523.

(14) Kumar, P.; Sarkar, P.; Stefi Raju, V.; Manikandan, V.; Guru, A.; Arshad, A.; Elumalai, P.; Arockiaraj, J. Pathogenicity and Pathobiology of Epizootic Ulcerative Syndrome (EUS) Causing Fungus *Aphanomyces invadans* and Its Immunological Response in Fish. *Rev. Fish. Sci. Aquacult.* **2020**, *28*, 358−375.

(15) Henrissat, B.; Callebaut, I.; Fabrega, S.; Lehn, P.; Mornon, J. P.; Davies, G. Conserved catalytic machinery and the prediction of a common fold for several families of glycosyl hydrolases. *Proc. Natl. Acad. Sci. U.S.A.* **1995**, *92*, 7090−7094.

(16) Davies, G.; Henrissat, B. Structures and mechanisms of glycosyl hydrolases. *Structure* **1995**, *3*, 853−859.

(17) Ravichandran, G.; Kumaresan, V.; Bhatt, P.; Arasu, M. V.; Al-Dhabi, N. A.; Arockiaraj, J. A Cumulative Strategy to Predict and Characterize Antimicrobial Peptides (AMPs) from Protein Database. *Int. J. Pept. Res. Ther.* **2017**, *23*, 281−290.

(18) Roy, S.; Maheshwari, N.; Chauhan, R.; Sen, N. K.; Sharma, A. Structure prediction and functional characterization of secondary metabolite proteins of Ocimum. *Bioinformation* **2011**, *6*, 315−319.

(19) Sannasimuthu, A.; Kumaresan, V.; Anilkumar, S.; Pasupuleti, M.; Ganesh, M. R.; Mala, K.; Paray, B. A.; Al-Sadoon, M. K.; Albeshr, M. F.; Arockiaraj, J. Design and characterization of a novel Arthrospira platensis glutathione oxido-reductase-derived antioxidant peptide GM15 and its potent anti-cancer activity via caspase-9 mediated apoptosis in oral cancer cells. *Free Radical Biol. Med.* **2019**, *135*, 198−209.

(20) Wei, L.; Ye, X.; Sakurai, T.; Mu, Z.; Wei, L. ToxIBTL: prediction of peptide toxicity based on information bottleneck and transfer learning. *Bioinformatics* **2022**, *38*, 1514−1524.

(21) Agrawal, P.; Bhagat, D.; Mahalwal, M.; Sharma, N.; Raghava, G. P. S.*AntiCP 2.0: An Updated Model for Predicting Anticancer Peptides*; BioRxiv, 2020. DOI: 10.1101/2020.03.23.003780.

(22) Velayutham, M.; Ojha, B.; Issac, P. K.; Lite, C.; Guru, A.; Pasupuleti, M.; Arasu, M. V.; Al-Dhabi, N. A.; Arockiaraj, J. NV14 from serine O-acetyltransferase of cyanobacteria influences the antioxidant enzymes in vitro cells, gene expression against H_2O_2 and other responses in vivo zebrafish larval model. *Cell Biol. Int.* **2021**, *45*, 2331−2346.

(23) Sarzaeem, A.; Mirakabadi, A. Z.; Moradhaseli, S.; Morovvati, H.; Lotfi, M. Cytotoxic effect of ICD-85 (venom-derived peptides) on HeLa cancer cell line and normal LK cells using MTT assay. *Arch. Iran. Med.* **2012**, *15*, 696−701.

(24) Al-Qubaisi, M.; Rozita, R.; Yeap, S. K.; Omar, A. R.; Ali, A. M.; Alitheen, N. B. Selective cytotoxicity of goniothalamin against hepatoblastoma HepG2 cells. *Molecules* **2011**, *16*, 2944−2959.

(25) Abdullah, A. S. H.; Mohammed, A. S.; Abdullah, R.; Mirghani, M. E. S.; Al-Qubaisi, M. Cytotoxic effects of *Mangifera indica* L. kernel extract on human breast cancer (MCF-7 and MDA-MB-231 cell lines) and bioactive constituents in the crude extract. *BMC Complementary Altern. Med.* **2014**, *14*, No. 199.

(26) Prabha, N.; Sannasimuthu, A.; Kumaresan, V.; Elumalai, P.; Arockiaraj, J. Intensifying the Anticancer Potential of Cationic Peptide Derived from Serine Threonine Protein Kinase of Teleost by Tagging with Oligo Tryptophan. *Int. J. Pept. Res. Ther.* **2020**, *26*, 75−83.

(27) Lakshmi, S.; Dhanya, G. S.; Joy, B.; Padmaja, G.; Remani, P. Inhibitory effect of an extract of Curcuma zedoariae on human cervical carcinoma cells. *Med. Chem. Res.* **2008**, *17*, 335−344.

(28) Sudhakaran, G.; Prathap, P.; Guru, A.; Rajesh, R.; Sathish, S.; Madhavan, T.; Arasu, M. V.; Al-Dhabi, N. A.; Choi, K. C.; Gopinath, P.; Arockiaraj, J. Anti-inflammatory role demonstrated both in vitro and in vivo models using nonsteroidal tetranortriterpenoid, Nimbin (N1) and its analogs (N2 and N3) that alleviate the domestication of alternative medicine. *Cell Biol. Int.* **2022**, *46*, 771−791.

(29) Sudhakaran, G.; Rajesh, R.; Guru, A.; Arasu, M. V.; et al. Nimbin analogs N5 and N7 regulate the expression of lipid metabolic genes and inhibit lipid accumulation in high-fat diet-induced zebrafish larvae: An antihyperlipidemic study. *Tissue Cell* **2022**, *80*, No. 102000.

(30) Sudhakaran, G.; Prathap, P.; Guru, A.; Rajesh, R.; Sathish, S.; Madhavan, T.; Arasu, M. V.; Al-Dhabi, N. A.; Choi, K. C.; Gopinath, P.; Arockiaraj, J. Anti-inflammatory role demonstrated both in vitro and in vivo models using non-steroidal tetranortriterpenoid, Nimbin (N1) and its analogues (N2 and N3) that alleviate the domestication of alternative medicine. *Cell Biol. Int.* **2022**, *24*, 327−332.

(31) Ahamed, M.; Alhadlaq, H. Nickel nanoparticle-induced dose-dependent cyto-genotoxicity in human breast carcinoma MCF-7 cells. *OncoTargets Ther.* **2014**, 269.

(32) Haridevamuthu, B.; Manjunathan, T.; Guru, A.; Kumar, R. S.; Rajagopal, R.; Kuppusamy, P.; Juliet, A.; Gopinath, P.; Arockiaraj, J. Hydroxyl containing benzo[b]thiophene analogs mitigates the acrylamide induced oxidative stress in the zebrafish larvae by stabilizing the glutathione redox cycle. *Life Sci.* **2022**, *298*, No. 120507.

(33) Manjunathan, T.; Guru, A.; Arokiaraj, J.; Gopinath, P. 6-Gingerol and Semisynthetic 6-Gingerdione Counteract Oxidative Stress Induced by ROS in Zebrafish. *Chem. Biodiversity* **2021**, *18*, No. e2100650.

(34) Haridevamuthu, B.; Guru, A.; Murugan, R.; Sudhakaran, G.; Pachaiappan, R.; Almutairi, M. H.; Almutairi, B. O.; Juliet, A.; Arockiaraj, J. Neuroprotective effect of Biochanin a against Bisphenol A-induced prenatal neurotoxicity in zebrafish by modulating oxidative stress and locomotory defects. *Neurosci. Lett.* **2022**, *790*, No. 136889.

(35) Guru, A.; Sudhakaran, G.; Almutairi, M. H.; Almutairi, B. O.; Juliet, A.; Arockiaraj, J. β-cells regeneration by WL15 of cysteine and glycine-rich protein 2 which reduces alloxan induced β-cell dysfunction and oxidative stress through phosphoenolpyruvate carboxykinase and insulin pathway in zebrafish in-vivo larval model. *Mol. Biol. Rep.* **2022**, *49*, 11867.

(36) Singh, M.; Guru, A.; Sudhakaran, G.; Pachaiappan, R.; Mahboob, S.; Al-Ghanim, K. A.; Al-Misned, F.; Juliet, A.; et al. Copper sulfate induced toxicological impact on in-vivo zebrafish larval model protected due to acacetin via anti-inflammatory and glutathione redox mechanism. *Comp. Biochem. Physiol., Part C: Toxicol. Pharmacol.* **2022**, *262*, No. 109463.

(37) Murugan, R.; Rajesh, R.; Seenivasan, B.; Haridevamuthu, B.; Sudhakaran, G.; Guru, A.; Rajagopal, R.; Kuppuswamy, P.; Juliet, A.; Gopinath, P.; Arockiaraj, J. Withaferin A targets the membrane of *Pseudomonas aeruginosa* and mitigates the inflammation in zebrafish larvae; an in vitro and in vivo approach. *Microb. Pathog.* **2022**, *172*, No. 105778.

(38) Al-Harbi, L. N.; Subash-Babu, P.; Binobead, M. A.; Alhussain, M. H.; AlSedairy, S. A.; Aloud, A. A.; Alshatwi, A. A. Potential Metabolite Nymphayol Isolated from Water Lily (*Nymphaea stellata*) Flower Inhibits MCF-7 Human Breast Cancer Cell Growth via Upregulation of Cdkn2a, pRb2, p53 and Downregulation of PCNA mRNA Expressions. *Metabolites* **2020**, *10*, No. 280.

(39) Siddhu, N. S. S.; Guru, A.; Satish Kumar, R. C.; Almutairi, B. O.; Almutairi, M. H.; Juliet, A.; Vijayakumar, T. M.; Arockiaraj, J. Pro-inflammatory cytokine molecules from Boswellia serrate suppresses lipopolysaccharides induced inflammation demonstrated in an in-vivo zebrafish larval model. *Mol. Biol. Rep.* **2022**, *49*, 7425−7435.

(40) Guru, A.; Sudhakaran, G.; Velayutham, M.; Murugan, R.; Pachaiappan, R.; Mothana, R. A.; Noman, O. M.; Juliet, A.; Arockiaraj, J. Daidzein normalized gentamicin-induced nephrotoxicity and associated pro-inflammatory cytokines in MDCK and zebrafish: Possible mechanism of nephroprotection. *Comp. Biochem. Physiol., Part C: Toxicol. Pharmacol.* **2022**, *258*, No. 109364.

(41) Sarkar, P.; Guru, A.; Raju, S. V.; Farasani, A.; Oyouni, A. A. A.; Alzahrani, O. R.; Athagafi, H. A. E.; Alharthi, F.; Karuppiah, K. M.; Arockiaraj, J. GP13, an Arthrospira platensis cysteine desulfurase-derived peptide, suppresses oxidative stress and reduces apoptosis in human leucocytes and zebrafish (*Danio rerio*) embryo via attenuated caspase-3 expression. *J. King Saud Univ., Sci.* **2021**, *33*, No. 101665.

(42) Issac, P. K.; Velayutham, M.; Guru, A.; Sudhakaran, G.; Pachaiappan, R.; Arockiaraj, J. Protective effect of morin by targeting mitochondrial reactive oxygen species induced by hydrogen peroxide demonstrated at a molecular level in MDCK epithelial cells. *Mol. Biol. Rep.* **2022**, *49*, 4269−4279.

(43) Guru, A.; Velayutham, M.; Arockiaraj, J. Lipid-Lowering and Antioxidant Activity of RF13 Peptide From Vacuolar Protein Sorting-Associated Protein 26B (VPS26B) by Modulating Lipid Metabolism and Oxidative Stress in HFD Induced Obesity in Zebrafish Larvae. *Int. J. Pept. Res. Ther.* **2022**, *28*, No. 74.

(44) Lite, C.; Guru, A.; Juliet, M.; Arockiaraj, J. Embryonic exposure to butylparaben and propylparaben induced developmental toxicity and triggered anxiety-like neurobehavioral response associated with oxidative stress and apoptosis in the head of zebrafish larvae. *Environ. Toxicol.* **2022**, *37*, 1988−2004.

(45) Haridevamuthu, B.; Guru, A.; Murugan, R.; Sudhakaran, G.; Pachaiappan, R.; Almutairi, M. H.; Almutairi, B. O.; Juliet, A.; Arockiaraj, J. Neuroprotective effect of Biochanin a against Bisphenol A-induced prenatal neurotoxicity in zebrafish by modulating oxidative stress and locomotory defects. *Neurosci. Lett.* **2022**, *790*, No. 136889.

(46) Sudhakaran, G.; Prathap, P.; Guru, A.; Haridevamuthu, B.; Murugan, R.; Almutairi, B. O.; Almutairi, M. H.; Juliet, A.; Gopinath, P.; Arockiaraj, J. Reverse pharmacology of Nimbin-N2 attenuates alcoholic liver injury and promotes the hepatoprotective dual role of improving lipid metabolism and downregulating the levels of inflammatory cytokines in zebrafish larval model. *Mol. Cell. Biochem.* **2022**, *477*, 2387−2401.

(47) Velayutham, M.; Guru, A.; Gatasheh, M. K.; Hatamleh, A. A.; Juliet, A.; Arockiaraj, J. Molecular Docking of SA11, RF13 and DI14 Peptides from Vacuolar Protein Sorting Associated Protein 26B Against Cancer Proteins and In vitro Investigation of its Anticancer Potency in Hep-2 Cells. *Int. J. Pept. Res. Ther.* **2022**, *28*, 1−12.

(48) Bai, C.-Z.; Feng, M.-L.; Hao, X.-L.; Zhao, Z.-J.; Li, Y.-Y.; Wang, Z.-H. Anti-tumoral effects of a trypsin inhibitor derived from buckwheat in vitro and in vivo. *Mol. Med. Rep.* **2015**, *12*, 1777−1782.

(49) Luo, X.; Zhu, W.; Ding, L.; Ye, X.; Gao, H.; Tai, X.; Wu, Z.; Qian, Y.; Ruan, X.; Li, J.; Li, S.; Chen, Z. Bldesin, the first functionally characterized pathogenic fungus defensin with Kv1.3 channel and chymotrypsin inhibitory activities. *J. Biochem. Mol. Toxicol.* **2019**, *33*, No. e22244.

(50) Soon, T. N.; Chia, A. Y. Y.; Yap, W. H.; Tang, Y.-Q. Anticancer Mechanisms of Bioactive Peptides. *Protein Pept. Lett.* **2020**, *27*, 823−830.

(51) Xie, M.; Liu, D.; Yang, Y. Anti-cancer peptides: classification, mechanism of action, reconstruction and modification. *Open Biol.* **2020**, *10*, No. 200004.

(52) Felício, M. R.; Silva, O. N.; Gonçalves, S.; Santos, N. C.; Franco, O. L. Peptides with Dual Antimicrobial and Anticancer Activities. *Front. Chem.* **2017**, *5*, No. 5.

(53) Chen, Z.; Wang, L.; Hong, D.; et al. Brevilaterin B from *Brevibacillus laterosporus* has selective antitumor activity and induces apoptosis in epidermal cancer. *World J. Microbiol. Biotechnol.* **2021**, No. 201.

(54) Emadi Shaibani, M.; Heidari, B.; Khodabandeh, S.; Shahangian, S. S. Production and Fractionation of Rocky Shore Crab (*Grapsus albacarinous*) Protein Hydrolysate by Ultrafiltration Membrane: Assessment of Antioxidant and Cytotoxic Activities. *J. Aquat. Food Prod. Technol.* **2021**, *30*, 339−352.

(55) Karanam, G.; Arumugam, M. K. Reactive oxygen species generation and mitochondrial dysfunction for the initiation of apoptotic cell death in human hepatocellular carcinoma HepG2 cells by a cyclic dipeptide Cyclo(-Pro-Tyr). *Mol. Biol. Rep.* **2020**, *47*, 3347−3359.

(56) Siddiqui, M. A.; Alhadlaq, H. A.; Ahmad, J.; Al-Khedhairy, A. A.; Musarrat, J.; Ahamed, M. Copper Oxide Nanoparticles Induced Mitochondria Mediated Apoptosis in Human Hepatocarcinoma Cells. *PLoS One* **2013**, *8*, No. e69534.

(57) Anderson, A. J.; Jackson, T. D.; Stroud, D. A.; Stojanovski, D. Mitochondria-hubs for regulating cellular biochemistry: emerging concepts and networks. *Open Biol.* **2019**, *9*, No. 190126.

(58) Rengarajan, T.; Keerthiga, S.; Duraikannu, S.; Periyannan, V. Exploring the anticancer and anti-inflammatory activities of ferruginol in MCF-7 breast cancer cells. *Cancer Plus* **2020**, 1.

(59) Al-Khayal, K.; Alafeefy, A.; Vaali-Mohammed, M.-A.; Mahmood, A.; Zubaidi, A.; Al-Obeed, O.; Khan, Z.; Abdulla, M.; Ahmad, R. Novel derivative of aminobenzenesulfonamide (3c) induces apoptosis in colorectal cancer cells through ROS generation and inhibits cell migration. *BMC Cancer* **2017**, *17*, No. 4.

(60) Rasaratnam, K.; Nantasenamat, C.; Phaonakrop, N.; Roytrakul, S.; Tanyong, D. A novel peptide isolated from garlic shows anticancer effect against leukemic cell lines via interaction with Bcl-2 family proteins. *Chem. Biol. Drug Des.* **2021**, *97*, 1017−1028.

(61) Kang, M. C.; Cha, S. H.; Wijesinghe, W. A. J. P.; Kang, S. M.; Lee, S. H.; Kim, E. A.; Song, C. B.; Jeon, Y. J. Protective effect of marine algae phlorotannins against AAPH-induced oxidative stress in zebrafish embryo. *Food Chem.* **2013**, *138*, 950−955.